

The Back-Projection Angular Flux Estimator

WILLIAM L. DUNN

Applied Research Associates, Inc., 4917 Professional Court, Raleigh, North Carolina 27609

Received August 16, 1984; revised January 15, 1985

A method of obtaining point angular flux estimates in Monte Carlo radiation transport calculations is presented. The method involves the back-projection of an area to define the volume within which interactions must occur in order to contribute to the desired angular flux and a limiting process to shrink the area to a line or a point. The approach is developed here by considering specific versions of the searchlight problem. Sample results generated using the estimator are given. © 1985 Academic Press, Inc.

INTRODUCTION

Various flux estimators have been developed for Monte Carlo radiation transport calculations [1-6]. Most of these estimators are based on physical principles and the definitions of flux or flux-related quantities. For instance, the reaction rate per unit volume is given by the product of scalar flux, Φ , and the appropriate macroscopic cross section, Σ , so that the so-called collision density estimator can be formed as

$$\hat{\Phi} = \frac{1}{NV\Sigma} \sum_{i=1}^N \sum_{j=1}^{v_i} W_{ij}, \quad (1)$$

where W_{ij} is the weight at the j th relevant collision in volume V during history i , v_i is the number of such collisions, and N is the number of histories. Similarly, the boundary crossing estimator,

$$\hat{\Phi} = \frac{1}{NA} \sum_{i=1}^N \sum_{j=1}^{v_i} \frac{W_{ij}}{\omega_{ij}}, \quad (2)$$

where ω_{ij} is the magnitude of the cosine of the angle between the normal to area A and the direction of particle history i during its j th path, results directly from the definition of current and its relation to flux.

Many existing estimators for obtaining angular flux at a point require that small, but finite, spatial and angular intervals be constructed through which the particles either migrate naturally (which is usually quite rare) or must be forced to migrate.

In either case, the flux quantity obtained is an average over finite intervals and truly point quantities are estimated by extrapolation, interpolation, or some similar means. For instance, we note that the denominators of Eqs. (1) and (2) contain, respectively, the volume V and area A of finite regions. As these quantities get smaller, the simulation becomes less efficient and in the limit as V and A tend to zero, the estimators lose their meaning.

Other estimators have been developed, such as the track-length, next-flight, and track rotation estimators, and a number of Monte Carlo codes have been written (e.g., MCNP and MORSE) that are capable of obtaining useful angular flux estimates. It is not our intention, however, to critically evaluate these existing estimators and codes (most have been treated extensively in the literature [1-8]) but rather to present an analysis that can be used to derive a new estimator for the angular flux in a given direction, Ω , that avoids the use of finite spatial (and/or angular) intervals in its final form. The estimator is called the back-projection angular flux estimator because it relies on projecting an area in the $-\Omega$ direction, thus describing the volume within which interactions must occur in order to contribute to the desired angular flux. One obtains point fluxes by employing a limiting process in order to shrink the area to a line or a point. Such an estimator can be useful, for instance, in estimating the exit angular flux at the boundaries of a medium, as we will show for one form of the searchlight problem, or at internal points.

ANALYSIS

The Monte Carlo method is based on general principles and theorems but its application is highly problem-specific. Viewed as a type of quadrature, its particular form (i.e., nodes and weights) can change dramatically from one problem to another. For this reason, we introduce the concept of the back-projection angular flux estimator by considering a particular, idealized application; we then discuss ways in which it can apply more generally.

To begin, we seek estimates of the exit normal flux at various, specified radial distances ρ , expressed in mean free paths, on the two surfaces of a uniform, plane-parallel slab of optical thickness τ , subject to a radiation beam incident normally to one surface at a point. The medium scatters isotropically and without inducing energy changes and there are no multiplicative or inelastic interactions so that the mean number of secondary particles per collision, c , is also the ratio of scatter to total cross sections. (This idealized problem was initially considered in order to verify a semianalytic solution that will be described in a subsequent paper.)

We construct a Cartesian reference frame whose origin is coincident with the point of incidence and whose positive z axis is parallel to the incident beam, as in Fig. 1. Particle position is specified in cylindrical coordinates (ρ, η, z) with η measured in the x, y plane counterclockwise from the positive x axis, and particle direction is specified by the unit vector Ω , which can be expressed in terms of the

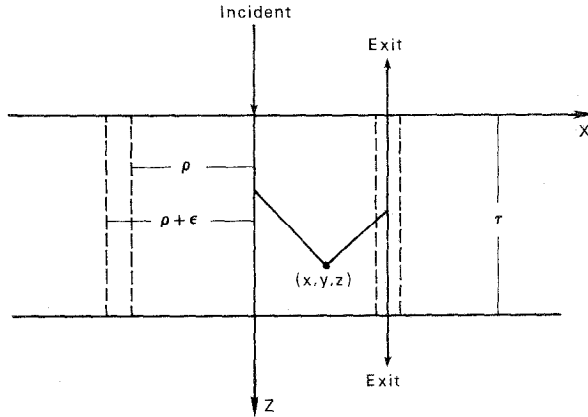


FIG. 1. Geometry for the exit normal flux estimator.

direction cosines (α, β, γ) or can be written $\Omega = \Omega(\gamma, \phi)$, with γ the z direction cosine and ϕ the azimuthal angle, also measured counterclockwise from the positive x direction. In order to construct our angular flux estimators, we consider the annular area between two imaginary circles with radii ρ and $\rho + \epsilon$ centered on the z axis on each of the boundary planes. By back-projecting these areas in directions opposite to the boundary outward normals, we obtain a volume between two concentric, right-circular cylinders (see Fig. 1) within which scatters must occur in order to contribute to the desired quantities; we call this volume the back-projected volume.

We let the estimators $\delta\hat{\Psi}_0$ and $\delta\hat{\Psi}_\tau$ represent the contributions after each scatter to the exit angular flux at $(\rho, \eta, 0)$ and (ρ, η, τ) , respectively, in the direction of the outward normal to each local surface. We construct these estimators by (a) extending the path from each scatter point (x, y, z) in the sampled direction Ω to its intersections (if any) with the annular region between the cylinders (in a next-flight sense), (b) forcing a "pseudo-scatter" there that directs the particle in an outward normal direction, (c) forcing the particle to escape, and (d) scoring with a boundary crossing estimator.

The term "pseudo-scatter" is used to mean a forced interaction within the back-projected volume that scatters the particle into the desired direction (in this case $\gamma = -1$ for $\delta\hat{\Psi}_0$ and $\gamma = 1$ for $\delta\hat{\Psi}_\tau$). We note that there can be zero, one, or two pseudo-scatter sites for any given photon path, depending on the number of intersections of the extended particle path with the back-projected volume.

In order to obtain point flux estimators, we take the limit as $\epsilon \rightarrow 0$ of the resulting expression, obtaining the general forms

$$\delta\hat{\Psi}_0 = \frac{WQ}{\omega_0} \lim_{\epsilon \rightarrow 0} \sum_{i=0}^v \frac{P_i(\epsilon) R_{i,0}}{A(\epsilon)}, \tag{3}$$

and

$$\delta\hat{\Psi}_\tau = \frac{WQ}{\omega_\tau} \lim_{\varepsilon \rightarrow 0} \sum_{i=0}^{\nu} \frac{P_i(\varepsilon) R_{i,\tau}}{A(\varepsilon)}, \quad (4)$$

where W is the incoming history weight; ν is the number of pseudo-scatter sites for the particular path; $P_i(\varepsilon)$ is the probability of reaching and then interacting at the i th pseudo-scatter site; Q is the probability of scattering into the unique direction that would allow the particle to exit normal to one of the boundary surfaces ($\gamma = -1$ for the $z=0$ surface and $\gamma = 1$ for the $z=\tau$ surface); $R_{i,0}$ and $R_{i,\tau}$ are the probabilities of reaching the surfaces at $z=0$ and $z=\tau$, respectively, from the i th pseudo-scatter site; $A(\varepsilon)$ is the area of the annular ring on either surface through which the exiting particles pass; and ω_0 and ω_τ are the cosines of the angles between the outward normals to the areas $A(\varepsilon)$ and the directions of the exiting particles. In the case being considered,

$$P_0(\varepsilon) = 0, \quad (5a)$$

$$P_1(\varepsilon) = e^{-D_{1+}} - e^{-D_{2+(\varepsilon)}}, \quad (5b)$$

and

$$P_2(\varepsilon) = e^{-D_{2-(\varepsilon)}} - e^{-D_{1-}}, \quad (5c)$$

where

$$D_{2\pm}(\varepsilon) = -\frac{\alpha x + \beta y}{\alpha^2 + \beta^2} \pm d(\varepsilon), \quad (6)$$

with

$$d(\varepsilon) = \left[\left(\frac{\alpha x + \beta y}{\alpha^2 + \beta^2} \right)^2 - \frac{x^2 + y^2 - (\rho + \varepsilon)^2}{\alpha^2 + \beta^2} \right]^{1/2}, \quad (7)$$

and

$$D_{1\pm} = D_{2\pm}(0). \quad (8)$$

Here, D_1 and $D_2(\varepsilon)$ are the distances from the interaction point in the direction Ω to the intersections with the cylinders at radii ρ and $\rho + \varepsilon$, respectively, as shown for one case in Fig. 2. We note that Eq. (6) gives the solutions to the quadratic equation that results from finding the intersections of the line

$$\frac{x_2 - x}{\alpha} = \frac{y_2 - y}{\beta} = D_2(\varepsilon) \quad (9)$$

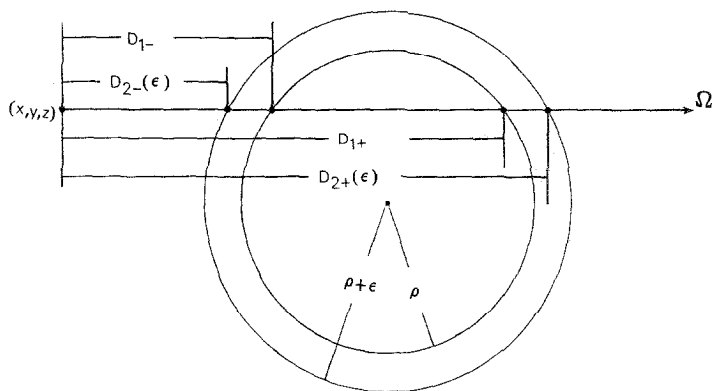


FIG. 2. The distances D_1 and D_2 for a particular case.

with the cylinder

$$x^2 + y^2 = (\rho + \epsilon)^2. \tag{10}$$

The remaining quantities in Eqs. (3) and (4) can be written

$$Q = \frac{c}{4\pi}, \tag{11}$$

since the scattering is isotropic,

$$R_{0,0} = R_{0,\tau} = 0, \tag{12a}$$

$$R_{1,0} = e^{-(z + \gamma D_{1+})}, \tag{12b}$$

$$R_{2,0} = e^{-(z + \gamma D_{1-})}, \tag{12c}$$

$$R_{1,\tau} = e^{-(\tau - z - \gamma D_{1+})}, \tag{12d}$$

$$R_{2,\tau} = e^{-(\tau - z - \gamma D_{1-})}, \tag{12e}$$

$$A(\epsilon) = 2\pi\rho\epsilon \tag{13}$$

and

$$\omega_0 = \omega_\tau = 1. \tag{14}$$

After substituting and applying l'Hôpital's rule, we obtain

$$\delta\hat{\Psi}_0 = 0, \quad v = 0, \tag{15a}$$

$$= \frac{Wc e^{-[z + D_{1+}(1 + \gamma)]}}{8\pi^2 (\alpha^2 + \beta^2) d_0}, \quad v = 1, \tag{15b}$$

$$= \frac{Wc e^{-[z + D_{1-}(1 + \gamma)]} + e^{-[z + D_{1+}(1 + \gamma)]}}{8\pi^2 (\alpha^2 + \beta^2) d_0}, \quad v = 2; \tag{15c}$$

and

$$\delta\tilde{\Psi}_\tau = 0, \quad v = 0, \quad (16a)$$

$$= \frac{Wc e^{-[\tau - z + D_{1+(1-\gamma)}]}}{8\pi^2 (\alpha^2 + \beta^2) d_0}, \quad v = 1, \quad (16b)$$

$$= \frac{Wc e^{-[\tau - z + D_{1-(1-\gamma)}]} + e^{-[\tau - z + D_{1+(1-\gamma)}]}}{8\pi^2 (\alpha^2 + \beta^2) d_0}, \quad v = 2, \quad (16c)$$

where

$$d_0 = d(0). \quad (17)$$

Equations (15) and (16) give the back-projection angular flux estimators for the exit normal fluxes at radius ρ for the considered searchlight problem. The estimators are independent of ε and hence give point angular flux estimates directly.

We suggest that the estimators of Eqs. (15) and (16) can be used in the following way. During simulation, force a scatter at each interaction site, with weight c ; the weight factor W will then have the value c^j after the j th interaction. At each scatter

TABLE I
Monte Carlo Estimates of the Exit Normal Fluxes

| ρ | Ψ_0 | $\sigma(\Psi_0)$ | Ψ_τ | $\sigma(\Psi_\tau)$ |
|--------|----------|------------------|-------------|---------------------|
| 0.001 | 5.49(0) | 4.5(-2) | 4.69(0) | 4.2(-2) |
| 0.01 | 5.43(-1) | 3.7(-3) | 4.65(-1) | 3.3(-3) |
| 0.1 | 4.60(-2) | 3.0(-4) | 4.11(-2) | 2.6(-4) |
| 0.2 | 1.97(-2) | 1.4(-4) | 1.82(-2) | 1.4(-4) |
| 0.4 | 7.44(-3) | 6.5(-5) | 7.08(-3) | 6.7(-5) |
| 0.6 | 3.76(-3) | 4.1(-5) | 3.60(-3) | 3.4(-5) |
| 0.8 | 2.17(-3) | 2.6(-5) | 2.12(-3) | 2.7(-5) |
| 1.0 | 1.32(-3) | 1.4(-5) | 1.29(-3) | 1.4(-5) |
| 1.2 | 8.79(-4) | 1.2(-5) | 8.59(-4) | 1.1(-5) |
| 1.4 | 5.71(-4) | 7.6(-6) | 5.64(-4) | 8.7(-6) |
| 1.6 | 4.01(-4) | 6.4(-6) | 3.98(-4) | 6.1(-6) |
| 1.8 | 2.65(-4) | 3.9(-6) | 2.63(-4) | 3.9(-6) |
| 2.0 | 1.98(-4) | 3.6(-6) | 1.95(-4) | 3.4(-6) |
| 2.2 | 1.40(-4) | 2.8(-6) | 1.38(-4) | 2.8(-6) |
| 2.4 | 1.05(-4) | 2.9(-6) | 1.02(-4) | 2.4(-6) |
| 2.6 | 7.06(-5) | 1.4(-6) | 7.11(-5) | 1.5(-6) |
| 2.8 | 5.46(-5) | 1.4(-6) | 5.60(-5) | 1.7(-6) |
| 3 | 4.18(-5) | 1.2(-6) | 4.15(-5) | 1.1(-6) |
| 4 | 1.01(-5) | 4.7(-7) | 1.10(-5) | 4.8(-7) |
| 5 | 2.54(-6) | 1.5(-7) | 2.55(-6) | 1.8(-7) |

Note. Ψ_0 and Ψ_τ are the exit normal fluxes on the $z=0$ and $z=\tau$ surfaces, respectively, for the case $c=0.8$ and $\tau=1$.

site, sample the scatter angles, update the direction cosines, score the angular flux with the back-projection estimator, pick the distance to the next interaction and continue as above until either the particle migrates from the medium or the history weight falls below some specified cutoff value.

We have used this approach to generate the results shown in Table I for the case $c = 0.8$ and $\tau = 1$. The FORTRAN 77 code was run on a Hewlett-Packard (HP) 1000 Model 6 microcomputer and 50,000 histories were simulated. Estimates of the exit normal fluxes and their sample standard deviations on both surfaces are shown; the numbers in parentheses are the exponents from the scientific notation representation.

GENERALIZATION

Presume that we now seek the exit angular flux in direction $\Omega_0 = (-\gamma_0, \eta)$, $\gamma_0 > 0$, at position (ρ, η) on the $z = 0$ surface for the geometry and incident distribution just considered. We back-project the annular area on the $z = 0$ surface in the $-\Omega_0$ direction, constructing an annular region between two hypothetical conic sections, as shown in Fig. 3. The back-projection angular flux estimator is of the same general form as Eq. (3) but some of the factors are different. The factor ω_0 becomes $\omega_0 = \gamma_0$ and the escape probabilities are of the slightly modified form

$$R_{0,0} = 0, \tag{18a}$$

$$R_{1,0} = e^{-(z + \gamma D_{1+})/\gamma_0}, \tag{18b}$$

and

$$R_{2,0} = e^{-(z + \gamma D_{1-})/\gamma_0}. \tag{18c}$$

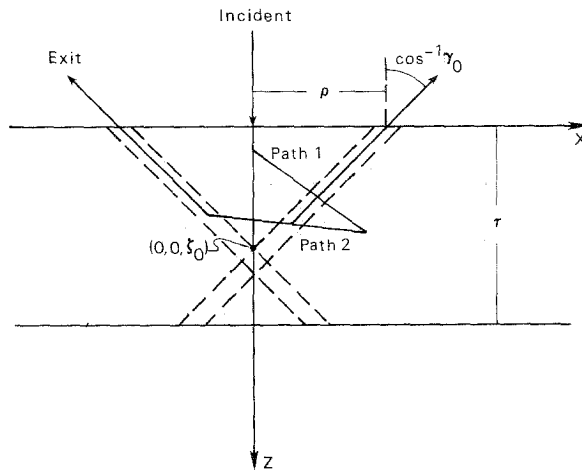


FIG. 3. Geometry for the exit flux estimator in direction $\Omega_0 = (-\gamma_0, \eta)$, with $\gamma_0 > 0$.

The probabilities of interacting within the region between conic sections depend on the order in which the conic sections are encountered (see paths 1 and 2 in Fig. 3). Thus,

$$P_0(\varepsilon) = 0, \quad (19a)$$

$$P_1(\varepsilon) = \pm [e^{-D_{1+}} - e^{-D_{2+(\varepsilon)}}], \quad (19b)$$

and

$$P_2(\varepsilon) = \pm [e^{-D_{1-}} - e^{-D_{2-(\varepsilon)}}], \quad (19c)$$

where the leading “+” sign is used if the conic section whose vertex is at $(0, 0, \zeta_0)$ is encountered first and the leading “-” sign is used otherwise. Here

$$\zeta_0 = \frac{\rho\gamma_0}{(1-\gamma_0^2)^{1/2}} = \frac{\rho}{T}, \quad (20)$$

with

$$T = \frac{(1-\gamma_0^2)^{1/2}}{\gamma_0}, \quad (21)$$

and the D_{\pm} values are determined from the intersections of a ray and the conic sections.

After substituting, taking the limit as $\varepsilon \rightarrow 0$, and applying l'Hôpital's rule, the flux estimator after each interaction is

$$\delta\hat{\Psi}_0 = 0, \quad v = 0, \quad (22a)$$

$$= \frac{Wc}{8\pi^2\rho\gamma_0} D_{0+} e^{-[D_{1+} + (z+\gamma D_{1+})/\gamma_0]}, \quad v = 1, \quad (22b)$$

$$= \frac{Wc}{8\pi^2\rho\gamma_0} \{ D_{0+} e^{-[D_{1+} + (z+\gamma D_{1+})/\gamma_0]} + D_{0-} e^{-[D_{1-} + (z+\gamma D_{1-})/\gamma_0]} \}, \quad v = 2 \quad (22c)$$

where

$$D_{1\pm} = -\xi_0 \pm d_0 \quad (23)$$

and

$$D_{0\pm} = |\xi'_0 \pm d'_0|, \quad (24)$$

with

$$\xi_0 = \frac{a_0\gamma(z - \zeta_0) - \alpha x - \beta y}{\alpha^2 + \beta^2 - a_0\gamma^2}, \tag{25}$$

$$d_0 = \left[\xi_0^2 - \frac{x^2 + y^2 - a_0(z - \zeta_0)^2}{\alpha^2 + \beta^2 - a_0\gamma^2} \right]^{1/2}, \tag{26}$$

$$a_0 = \frac{\rho^2}{\zeta_0^2} = T^2, \tag{27}$$

$$\xi'_0 = \frac{-a_0\gamma}{T(\alpha^2 + \beta^2 - a_0\gamma^2)}, \tag{28}$$

and

$$d'_0 = \frac{\xi_0 \xi'_0}{d_0} - \frac{a_0(z - \zeta_0)}{T d_0(\alpha^2 + \beta^2 - a_0\gamma^2)}. \tag{29}$$

A similar analysis can be used to generate $\delta\hat{\Psi}_\tau$ for this case. The result is of the same form as Eqs. (22) with all $(z + \gamma D_1)$ quantities replaced by $(\tau - z - \gamma D_1)$ terms.

We note that in the limiting case as $\gamma_0 \rightarrow 1$, it is a simple matter to show that $T \rightarrow 0$, $a_0 \rightarrow 0$, $\zeta_0 \rightarrow \infty$, and $D_{0\pm} \rightarrow \pm \rho / [(\alpha^2 + \beta^2) d_0]$, so that Eqs. (22) reduce to Eqs. (15) for the exit normal flux estimator.

We note further that incident particles entering the medium at $(0, 0, 0)$ with $\alpha = \beta = 0$ and $\gamma = 1$ must scatter at the point $(0, 0, \zeta_0)$, the vertex of the conic section, in order to exit at (ρ, η) in the direction Ω_0 after only one interaction. The single-scatter component of the angular flux can be obtained from Eq. (22) by letting $\alpha = \beta = 0$ and taking the limit as $\gamma \rightarrow 1$, which yields, for $0 < \gamma_0 < 1$,

$$\Psi_1(\rho, \eta, 0, -\gamma_0, \eta) = \frac{c}{8\pi^2 \rho \gamma_0 T} e^{-\zeta_0(1 + 1/\gamma_0)}, \quad \rho < \tau T \tag{30a}$$

$$= 0, \quad \rho > \tau T. \tag{30b}$$

This result is equivalent to that of Siewert and Dunn [9], developed by the F_N method, for the single-scatter component from a half-space subject to the incident angular flux $\Psi(\rho, \eta, 0, \gamma, \phi) = \delta(\rho)\delta(\gamma - 1)\delta(\phi - \phi_0)/(2\pi\rho)$, $\gamma > 0$.

The estimator of Eqs. (22) was used to give the results shown in Table II for the case $c = 0.8$, $\tau = 1$, and $\gamma_0 = 0.5$. These results were generated by a FORTRAN 77 code run on the HP 1000 Model 6 in which 20,000 histories were simulated. Also shown in Table II are the sample standard deviations and the single-scatter components calculated from Eqs. (30).

The back-projection estimator can be used to obtain energy- or frequency-dependent fluxes in the standard Monte Carlo manner by scoring over finite energy or

TABLE II
 Monte Carlo Estimates of the Exit Angular Flux

| ρ | Ψ | $\sigma(\Psi)$ | Ψ_1 |
|--------|----------|----------------|----------|
| 0.001 | 2.77(1) | 1.8(0) | 1.17(1) |
| 0.01 | 2.74(0) | 1.7(-1) | 1.15(0) |
| 0.1 | 2.54(-1) | 1.7(-2) | 9.84(-2) |
| 0.2 | 1.16(-1) | 8.0(-3) | 4.14(-2) |
| 0.4 | 6.18(-2) | 1.3(-2) | 1.46(-2) |
| 0.6 | 3.27(-2) | 6.5(-3) | 6.90(-3) |
| 0.8 | 1.95(-2) | 3.9(-3) | 3.66(-3) |
| 1.0 | 1.30(-2) | 2.7(-3) | 2.07(-3) |
| 1.2 | 8.31(-3) | 1.9(-3) | 1.22(-3) |
| 1.4 | 4.49(-3) | 1.1(-3) | 7.39(-4) |
| 1.6 | 2.00(-3) | 1.7(-4) | 4.58(-4) |
| 1.8 | 9.72(-4) | 1.2(-4) | 0.00 |
| 2.0 | 6.11(-4) | 7.6(-5) | 0.00 |
| 2.2 | 3.87(-4) | 4.8(-5) | 0.00 |
| 2.4 | 2.31(-4) | 1.1(-5) | 0.00 |
| 2.6 | 2.09(-4) | 4.0(-5) | 0.00 |
| 2.8 | 1.77(-4) | 3.9(-5) | 0.00 |
| 3 | 1.41(-4) | 3.5(-5) | 0.00 |
| 4 | 3.48(-5) | 1.1(-5) | 0.00 |
| 5 | 5.63(-6) | 1.3(-6) | 0.00 |

Note. Ψ , and the once-scattered component, Ψ_1 , on the $z=0$ surface for the case $c=0.8$, $\tau=1$, $\gamma_0=0.5$, and $\phi=\eta$.

frequency intervals. Also, it is a simple matter to extend the analysis to the anisotropic case by replacing $Q = c/(4\pi)$ by

$$Q = \frac{1}{\Sigma_t} \frac{d\Sigma_s}{d\Omega}(\mathbf{\Omega} \rightarrow \mathbf{\Omega}_0), \quad (31)$$

where $d\Sigma_s/d\Omega$ is the differential scattering cross section, $\mathbf{\Omega}$ is the direction from the real scatter point to the pseudo-scatter point, $\mathbf{\Omega}_0$ is the direction in which the angular flux estimate is desired and Σ_t is the total cross section. Although we have expressed our estimators for fluxes at the boundaries, they apply equally well at internal points; it is simply necessary to convert the escape probabilities $R_{i,0}$ and $R_{i,\tau}$ to expressions that describe the probabilities of reaching the appropriate internal points.

We expect that the method can be extended to obtain estimators for the angular flux in arbitrary directions at arbitrary positions and we intend to investigate this possibility in future work.

CONCLUSIONS

The back-projection angular flux estimator employs a limiting process before the simulation, obviating the need to find average flux values over finite spatial and angular intervals. The analysis has been used to develop certain surface angular flux estimates for the searchlight problem, with normal incidence and under some restrictions on azimuthal symmetry. It is hoped that these symmetry restrictions can be relaxed in future work. It is noted that use of the back-projection estimator makes possible certain analytic results, such as Eq. (30a), without the need to perform any simulations.

The main virtue of this approach is that the form of the estimator is independent of angular or spatial interval sizes and hence the estimator provides an efficient means to estimate point angular fluxes directly. The ability to estimate angular flux at a point is useful in a variety of radiation transport calculations. For instance, in x -ray imaging work (such as computed tomography), the process of designing collimators to reduce the scattered radiation contribution to the detector response could benefit from a knowledge of the angular flux distribution exiting the object to be imaged. Also, in active remote sensing applications where a directed microwave beam is incident on a medium, the angular distribution of the transmitted and/or backscattered radiation is dependent on certain properties of the medium. Methods for estimating that angular distribution could be helpful in designing models to infer these properties.

The major restriction of the method as it has been applied here is that it applies only on lines of symmetry (circles in the x - y plane) and that it requires that the azimuthal direction angle, ϕ , be equal to the spatial azimuthal angle, η . The extension to more general cases would appear in principal to be possible, though geometrically complex. In any event, the estimator is efficient and useful for the cases discussed.

ACKNOWLEDGMENTS

The material in this paper was influenced by Dr. C. E. Siewert, who developed a formula equivalent to Eq. (30a) for the single-scatter contribution to the exit angular flux for the searchlight problem with normal incidence on a half space, and by Drs. J. H. Renken and J. E. Morel of Sandia Laboratories, who contributed an independent derivation of that result. Part of this work was supported by the National Science Foundation under Grant CPE-8360797.

REFERENCES

1. M. H. KALOS, *Nucl. Sci. Eng.* **16** (1963), 111.
2. D. B. MACMILLAN, *Nucl. Sci. Eng.* **26** (1966), 366.
3. E. M. GELBARD, L. A. ONDIX II, AND J. SPANIER, *SIAM J. Appl. Math.* **14** (1966), 697.
4. J. SPANIER, *SIAM J. Appl. Math.* **14** (1966), 702.
5. H. A. STEINBERG AND M. H. KALOS, *Nucl. Sci. Eng.* **44** (1971), 406.

6. A. DUBI, Y. S. HOROWITZ, AND H. RIEF, *Nucl. Sci. Eng.* **71** (1979), 29.
7. E. A. STRAKER, W. H. SCOTT, AND N. R. BYRN, "The MORSE General Purpose Monte Carlo Multigroup Neutron and Gamma-Ray Transport Code with Combinatorial-Geometry," USAEC Report ORNL-4585, (1970).
8. LOS ALAMOS MONTE CARLO GROUP, "MCNP—A General Monte Carlo Code for Neutron and Photon Transport," LA-7396-M, revised, 1981.
9. C. E. SIEWERT AND W. L. DUNN, *Z. Angew. Math. Phys.* **34** (1983), 627.